Original Article
Food Science and Technology

ISSN 0101-2061 (Print)
ISSN 1678-457X (Online)

DOI: https://doi.org/10.1590/fst.88122



# The structures and catalytic behaviors of two new complexes based on bifunctional tetrazole-carboxylate connector

Dandan ZHAO[1*], Yang ZHAO[1], Huiqin ZHANG[2], Sujiao HE[1], Zhuanghong CAI[1], Luhong HE[1]

**Abstract**

Two transition metal coordination complexes $[Co(Tppebc)_2(Py)(H_2O)]_n$ (**1**) and $[Ni(Tppebc)_2(Py)(H_2O)]_n$ (**2**) (Py = pyridine, Tppebc = 3-(4-(2-(1H-tetrazol-5-yl)phenyl-4-yl) phenyl)-2-ethoxy-3H-benzimidazole-4-carboxylic acid) have been prepared by a hydrothermal method. The structural unit of complexes **1** and **2** adopts similar distorted octahedra geometry. Furthermore, both of those complexes feature a 1D chain and can be further extended to a higher-dimensional architecture through π···π stacking and hydrogen bonding. The catalytic property of complexes **1** and **2** were researched in the green catalytic process of the oxidative 2,6-di-*tert*-butylphenol (DBP). The high conversion and good selectivity results strongly indicate that both of the title complexes are catalytically active under the optimized reaction conditions.

**Keywords:** tetrazole-carboxylate connector; crystal structures; 1D chains; catalytical active.

**Practical Application:** Two novel metal complexes based on Co and Ni have been synthesized and demonstrated that they feature good catalytic property in the green catalytic process. These complexes have great potential to be applied as a class of novel catalysis in the synthetic and industrial chemistry.

## 1 Introduction

Enormous attentions have been paid to coordination complexes, because of diverse fascinating functionalities and excellent applications, such as catalysis, luminescence, molecular magnetism and conductivity (Liu et al., 2017; Chang et al., 2011; Feng et al., 2010; Pan et al., 2011). Among thousands of coordination complexes investigated, a significant number of them are appropriative to the rational design of intriguing structural motifs with rich physical and chemical performances using multidentate organic ligands such as N-heterocyclic ligands and carboxylate ligands (Burrows et al., 2011; Cheng et al., 2012; Yang et al., 2009). Recently, considerable efforts have been made on the architectures of complexes according to the tetrazole and imidazole derivates (Li et al., 2009; Ni et al., 2011). Among them, 5-substituted tetrazoles turn out to be an excellent class of building blocks in the synthesis of structurally versatile complexes, which can strongly tune properties and performances of complexes (Pachfule et al., 2010; Qiu et al., 2010). Tetrazolyl-carboxylate ligands as excellent building blocks bearing various coordination modes and variable configurations, can give rise to intriguing MOFs with beautiful aesthetics and useful functionalization (Naik et al., 2010; Zhang et al., 2013). Accordingly, the tetrazole-carboxylate derivative 3-(4-(2-(1H-tetrazol-5-yl) phenyl-4-yl) phenyl)-2-ethoxy-3H-benzimidazole-4-carboxylic acid (Tppebc) is a good candidate for greater tunability of structural frameworks. It is well-known that coordination complexes based on mixed-ligands exhibit unusual architectures, as combining different ligands could satisfy the coordination geometries requirement of metal centers during the assembly procedure (Guo et al., 2019; Geng et al., 2022; Kanoo et al., 2009). It is worth noting that the proficient introduction of the neutral pyridine analogs as auxiliary ligands into the reaction systems involving multifarious carboxylic acid ligands was concerned in recent years, which may form attractive coordination architectures (Kumar et al., 2006; Zhang et al., 2013).

Taking the above-mentioned factors into considerations, the two novel complexes $[Co(Tppebc)_2(Py)(H_2O)]_n$ (**1**) and $[Ni(Tppebc)_2(Py)(H_2O)]_n$ (**2**) have been prepared through the reaction of corresponding $Co^{II}$/ $Ni^{II}$ salts with the primary ligand Tppebc and the auxiliary ligand pyridine under similar hydrothermal conditions. The results manifest that the coordination modes of tetrazole moiety and pyridine can significantly affect the structure of complexes. In addition, the catalysis–structure relationships indicate that the coordinated environments of the $Co^{II}$/$Ni^{II}$ centers play a vital role in their catalytic activities.

## 2 Experimental

### *2.1 Materials and measurements*

All chemical reagents were purchased from commercial sources and directly used. The elemental composition of complexes **1** and **2** were performed on a Flash EA 1112 elemental analyzer. Infrared radiation (IR) data spectra were measured on a BRUKER TENSOR 27 spectrophotometer. Thermogravimetric analysis was performed on a METTLER TOLEDO TGA/SDTA instrument under a nitrogen atmosphere

*Received 01 Aug., 2022*
*Accepted 19 Sept., 2022*
[1] *College of Chemical Engineering, Henan Vocational College of Applied Technology, Zhengzhou, China*
[2] *College of Materials and Chemical Engineering, Zhongyuan University of Technology, Zhengzhou, China*
*Corresponding author: zhaodandan613@163.com

upon 10 °C·min$^{-1}$ heating rate. The X-ray diffraction data was recorded on a SuperNova with graphite mono-chromated Cu-Kα radiation (λ = 1.54184 Å).

### *2.2 Synthesis of [Co(Tppebc)(Py)($H_2O$)]$_n$ (1)*

Firstly, 0.0146 g $Co(NO_3)_2.6H_2O$ (0.05 mmol), 0.0220 g Tppebc (0.05 mmol) and 1 mL pyridine was treated by water (4 mL) and methanol (8 mL) mixture solution. The reaction was performed in a Teflon-lined stainless-steel container (25 mL) for 3 days at 150 °C. Then, the reaction medium was gradually cooled at a rate of 5 °C·h$^{-1}$. The product was obtained as a pink rhombic block crystal. Yield: 55% (based on Co). Elemental analysis (%) calcd for $C_{27}H_{21}CoN_7O_4$: C, 57.25; H, 3.74; N, 17.31. Found: C, 57.12; H, 3.93; N, 17.26. IR(KBr/pellet; ν, cm$^{-1}$): 3375(m), 1698(s), 1604(w), 1570(s), 1489(w), 1452(m), 1396(s), 1301(w), 1141(m), 1070(m), 957(w), 814(w).

### *2.3 Synthesis of [Ni(Tppebc)(Py)($H_2O$)]$_n$ (2)*

The synthetic procedure of **2** is similar with that of complex **1**. Briefly, 0.0145 g $Ni(NO_3)_2.6H_2O$ (0.05 mmol) was replaced with equimolar of $Co(NO_3)_2.6H_2O$. The complex **2** was synthesized as a green block crystal. Yield: 63% (based on Ni). Elemental analysis (%) calcd for $C_{27}H_{21}NiN_7O_4$: C, 57.28; H, 3.74; N, 17.32. Found: C, 57.33; H, 3.69; N, 17.16. IR(KBr/pellet; ν, cm$^{-1}$): 3207(m), 1700(s), 1619(m), 1571(s), 1490(w), 1450(m), 1302(w), 1188(w), 1219(w), 1023(m), 997(w), 760(m).

### *2.4 Crystal structure determination*

The suitable crystal chunks of complexes **1** and **2** were equipped mounted on glass fibres and then they were measured on a Super Nova with graphite mono-chromated Cu-Kα radiation (λ = 1.54184 Å) at 293(2) K. The structures of complexes **1** and **2** were analyzed via direct methods and expanded with Fourier techniques (Martins et al., 2019). The structural refinements were performed on an OLEX2 crystallographic program (Dolomanov et al., 2010). Crystal data containing space group, lattice parameters and other relevant information for the title complexes are listed in Table 1. Relevant bond lengths and bond angles are summerized in Table 2.

### *2.5 Catalytic reactions*

Complex **1** was choosed as a represent catalyst under the optimized reaction conditions, in which 0.02 mmol of the catalyst and 1 mmol of the co-catalyst $NaOCH_3$ was added to different reaction mediums and stirred at 45 °C. Afterwards, 200 μL of $H_2O_2$ (of 30% aqueous solution) was gradually added into the mixture at an interval of 25 minutes (four times in all) to minimize the decomposition of $H_2O_2$. After 3 h, the mixture was condensed in vacuum, and the products were separated out by preparative TLC conducted on dry silica gel plates with dichloromethane–petroleum ether (1:4 v/v) as the elution solvents. The products were gathered and arid in vacuo. The main product, 3,3',5,5'-tetra-tert-butyl-4,4'-diphenoquinone (DPQ): IR(cm$^{-1}$): 3439(m), 3010(w), 2960(s), 2864(m), 1608(s), 1460(m), 1267(w), 1090(s), 1038(m), 847(w). The byproduct: 2,6-ditert-butylbenzoquinone (BQ), IR(cm$^{-1}$): 3301(w), 2959(m), 2870(m), 1653(s), 1560(m), 1321(m), 1243(w), 1081(m), 920(m), 819(w).

**Table 1**. Crystal data and structure refinement for complexes **1** and **2**.

| Complex | **1** | **2** |
|---|---|---|
| Empirical formula | $C_{27}H_{21}CoN_7O_4$ | $C_{27}H_{21}NiN_7O_4$ |
| Formula weight | 566.44 | 566.22 |
| Temperature (K) | 293(2) | 293(2) |
| Wavelength (Mo-Kα) (Å) | 1.54184 | 1.54184 |
| Crystal system | triclinic | triclinic |
| Space group | P-1 | P-1 |
| *a* | 8.1543(3) | 8.0870(3) |
| *b* | 11.5919(5) | 11.6192(5) |
| *c* | 13.3086(6) | 13.2622(6) |
| α | 97.015(4) | 97.320(4) |
| β | 94.562(3) | 94.120(3) |
| γ | 99.713(3) | 100.042(3) |
| Volume (Å$^3$), Z | 1224.20(9), 2 | 1211.43(9), 2 |
| *F* (000) | 582 | 584 |
| θ range for data collection(o) | 3.36 to 73.52 | 3.38 to 73.49 |
| Goodness-of-fit on $F^2$ | 1.071 | 1.026 |
| Final $R_1$[a], $wR_2$[b] | 0.0342, 0.0886 | 0.0344, 0.0884 |

[a]$R_1 = [|F_0|-|F_c|]/|F_0|$; [b]$wR_2 = [w(F_0^2-F_c^2)^2]/[w(F_0^2)^2]^{1/2}$. $w = 1/[\sigma^2(F_o)^2+0.0297\,P^2+27.5680P]$, where $P = (F^2_o+2F^2_c)/3$.

**Table 2**. Selected bond lengths and angles for complexes **1** and **2.**

| Complex **1** | | | |
|---|---|---|---|
| Co(1)-O(1) #1 | 2.0572(14) | Co(1)-O(2) | 2.1144(13) |
| Co(1)-O(3) | 2.2086(15) | Co(1)-N(2)#2 | 2.1069(16) |
| Co(1)-N(3)#1 | 2.1486(16) | Co(1)-N(7) | 2.1466(17) |
| 3#Co(1)-N(2) | 2.1069(16) | 1#Co(1)-N(3) | 2.1486(16) |
| 1#O(1)-Co(1)-O(2) | 97.42(5) | 1#O(1)-Co(1)-O(3) | 87.71(6) |
| 1#O(1)-Co(1)-N(3)#1 | 88.70(6) | 1#O(1)-Co(1)-N(7) | 175.54(6) |
| O(2)-Co(1)-O(3) | 85.81(5) | O(2)-Co(1)-N(3)#1 | 169.94(6) |
| O(2)-Co(1)-N(7) | 87.00(6) | 2#N(2)-Co(1)-O(2) | 92.17(6) |
| 2#N(2)-Co(1)-N(3)#1 | 96.29(6) | 1# N(3)-Co(1)-O(3) | 86.47(6) |
| Complex **2** | | | |
| 1#Ni(1)-O(1) | 2.0473(14) | Ni(1)-O(2)#2 | 2.1231(13) |
| 1#Ni(1)-O(3) | 2.1283(14) | 1#Ni(1)-N(4)#2 | 2.0583(16) |
| 1#Ni(1)-N(5) | 2.0949(16) | 1#Ni(1)-N(7) | 2.0925(17) |
| 1#Ni(1)-O(2) | 2.1231(13) | 2#Ni(1)-N(4) | 2.0583(16) |
| O(1)-Ni(1)-O(2)#1 | 95.52(6) | O(1)-Ni(1)-O(3) | 87.61(6) |
| O(1)-Ni(1)-N(4)#2 | 84.49(6) | O(1)-Ni(1)-N(5) | 88.43(6) |
| 2#N(4)-Ni(1)-O(2) #1 | 91.56(6) | 1#O(2)-Ni(1)-O(3) | 85.26(5) |
| 2#N(4)-Ni(1)-O(3) | 171.17(6) | 2#N(4)-Ni(1)-N(5) | 96.03(6) |
| 2#N(4)-Ni(1)-N(7) | 95.22(7) | N(5)-Ni(1)-O(2)#1 | 171.76(6) |
| N(7)-Ni(1)-O(2)#1 | 87.80(6) | N(7)-Ni(1)-N(5) | 88.30(7) |

Symmetry transformations used to generate equivalent atoms: #3 1+X,+Y,+Z for **1**; #1-X,1-Y,-Z; #2 1-X,1-Y,-Z for **2**.

## 3 Results and discussions

### *3.1 Crystal structure of [Co(Tppebc)(Py)($H_2O$)]$_n$ (1)*

The unit of this complex includes one Co(II) center, one Tppebc, one pyridine and one water. As illustrated in Figure 1, the Co(II) center features a six-coordinated mode with a distorted octahedra geometry, coordinating with two N atoms (N2, N3) from two Tppebc, one N atom (N7) from pyridine and two O atoms (O1, O2) from another two Tppebc and O3 atom from the coordinated water molecular. The bonding lengths of Co–O and Co–N are ranging from 2.0572 to 2.2086 Å, which are in accordance with those previously observed in other Co(II) complexes (Bai et al., 2010; Yang et al., 2009). Bridging by two carboxylate groups from two Tppebc ligands, every two adjacent Co(II) metal centers are constructed into a binuclear unit, which are extended by Tppebc to result in a 1D chain (Figure 2).

In addition, the structure of complex **1** is further stabilized by face-to-face π···π interactions between the pyridine ring and imidazole ring with centroid separation of 3.6257(16) Å and the dihedral angle of 7.70(14)°. C–H···π interaction between the C5 atom and the centroid of benzene is existed with the separation of 3.628(2) Å. Moreover, adjacent 1D chains are stabilized through strong hydrogen bonds (O4···N6, 2.877(2) Å; O3···O2, 2.834(2) Å; O3···N4, 2.752(2) Å; C9–···O2, 2.989(2) Å; C9–O4, 2.858(2) Å). Thus, complex **1** is finally formed a 3D supra-molecular structure by π···π interactions and hydrogen bonds (Figure 3).

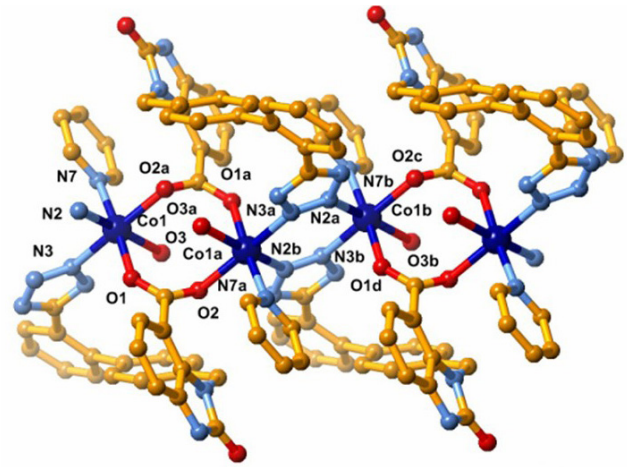


**Figure 1.** Schematic illustration of the crystal structure of **1**.

### *3.2 Crystal Structure of [Ni(Tppebc)(Py)($H_2O$)]$_n$ (2)*

When the Co(II) center was replaced by Ni(II) center, a similar 1D coordination complex **2** was obtained. The asymmetric unit consists of a Ni(II) center, one Tppebc, one pyridine and one water. As shown in Figure 4, the Ni(II) center displays a slightly distorted octahedral geometry, including two tetrazole nitrogen atoms, one pyridine nitrogen atom, two carboxylate oxygen atoms, and one water oxygen atom. Both Ni–N and Ni–O distances are located in the similar scope with those in other Ni(II) complexes (Ghannam et al., 2018; Zianna et al., 2016). Each Tppebc ligand applies two oxygen atoms from two carboxylate ligands to bridge two Ni(II) centers, constructing a large Ni–Tppebc–Ni–Tppebc ellipse hole with Ni1···Ni1 distance of 4.5130(5) Å. In addition, the Ni(II) centers are connected by Tppebc to result in a 1D chain (Fig. S1).

For imidazole ring and pyridine ring, the centroid-tocentroid separation distance is 3.6096(15) Å with a dihedral angle of 8.18(14)°. The separation of the C–H···π force between the centroid of benzene and the C5 is 3.622(3) Å. Besides, the 1D chains are benefited from the hydrogen bonds (O4···N1, 2.880(2) Å; O3···O2, 2.760(2) Å; C9···O2, 2.997(2) Å; C15·· N2, 2.927(3) Å; C9···O4, 2.857(3) Å). From hydrogen-bonding and π···π interactions, complex **2** is finally connected into a 3D supra-molecular framework (Fig. S2).

### *3.3 Thermal analyses*

Both compounds **1** and **2** were maintained and are able to maintain stability in ambient condition. Complex **1** remains stable until 201 °C with two exothermic peaks at 314, 490 °C through the DSC curve, indicating the decomposition of this

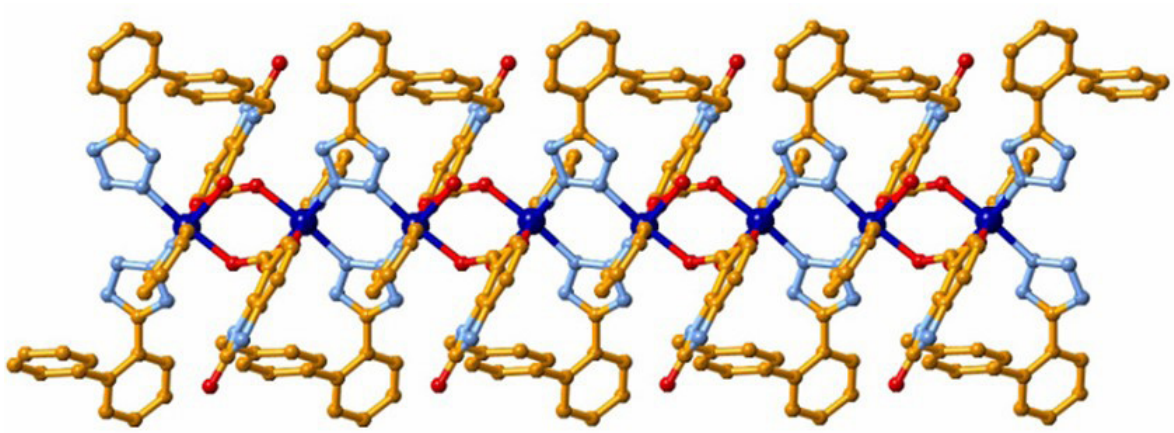

**Figure 2.** Schematic illustration of the 1D chain structure of **1**.

complex (Fig. S3). As for **2**, it was rather at 277 °C. The DSC demonstrated that there was an exothermic peak at around 503 °C, illustrate sing the framework decomposition (Fig. S4).

### *3.4 Catalytic properties of complexes*

In recent years, the application of MOFs as catalysts has gained a great number of research attentions, since MOFs are featured with following advantages: 1) the controllable oxidation state and electron density of metal center can be introducing different ligands, associating with selectivity coordinated geometry and catalytic behaviors (Lan et al., 2019; Wang et al., 2015). Therefore, we studied the catalytic behaviors of **1** and **2** with DBP clean oxidant $H_2O_2$ as oxidant together with $NaOCH_3$ as co-catalyst in different solvents at a certain temperature (Hu et al., 2012; Kennemur et al., 2019). The standard reaction system of DBP selective catalytic substrate $H_2O_2$ oxidation was selected in this work (Scheme S1, Supplementary Material). The relevant catalytic results are summarized in Table 3 and Table 4. Regarding to those experimental data, the catalytic substrate reaction is strongly dependent on the applied solvent, among which acetonitrile turned out to be the suitable reaction medium, in accordance with other papers reported before (Santos et al., 2020). DBP was oxidized by complexes **1** and **2** with $H_2O_2$ as oxidant, respectively, resulting in the coupled main product DPQ and the by-product BQ. Under the optimized reaction medium, the yield of rates of both complexes **1** and **2** were 81% and 80%, respectively. Also, the conversion rate of DBP is approximately 90% for the two catalytic substrate reaction. Importantly, the experiment to oxidize DBP only in the presence of $H_2O_2$ resulting in much less catalytic product (35% or 64%, respectively), in line with previous reports (Turk et al., 2005; Mu et al., 2011). These results illustrate that complexes **1** and **2** are featured with high catalytic activity to synthesize di-benzoquinone product. In addition, complexes **1** and **2** manifest similar catalytic activities under the same reaction conditions, owning to their same geometric configurations.

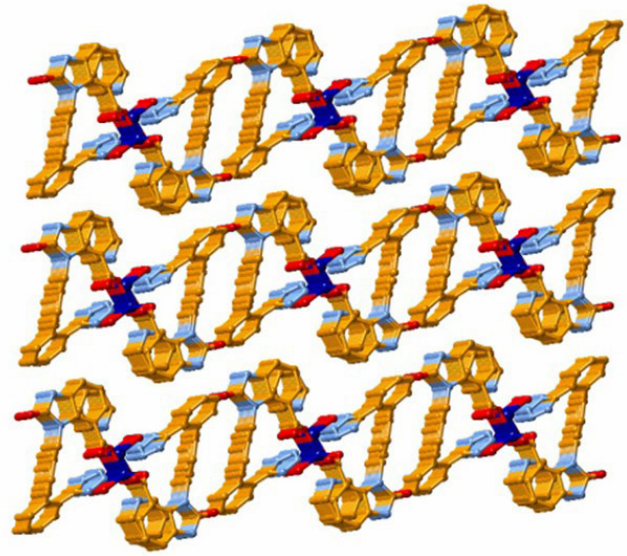

**Figure 3.** Schematic illustration of 3D supra-molecular structure of **1**.

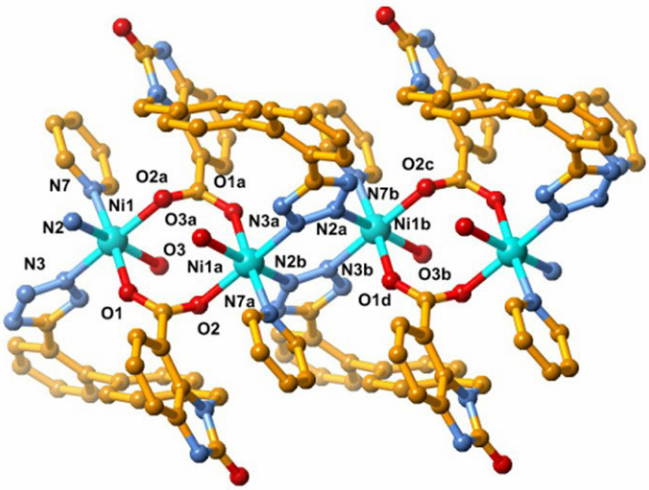


**Figure 4.** Schematic illustration of the crystal structure of **2**.

**Table 3.** The catalytic activity analyses of complex **1** with DBP[A].

| Solvent | Acetone | Methanol | Ethanol | Acetonitrile | Water |
|---|---|---|---|---|---|
| Conversion of DBP (%) | 93 | 89 | 85 | 95 | 86 |
| Yield (%)[B] DPQ | 81 | 79 | 73 | 87 | 76 |
| Yield (%)[B] BQ | 9 | 7 | 9 | 6 | 8 |
| Selectivity[C] DPQ (%) | 90 | 92 | 89 | 94 | 90 |

[A]Reaction conditions: 1 mmol of DBP and $NaOCH_3$, 0.02 mmol of catalyst and 20 μL of $H_2O_2$ in 2 mL reaction medium at 45 °C; [B]Conversions and yield rates for DPQ; [C]Selectivity = ([DPQ]×100)/([DPQ] + [BQ]).

**Table 4.** The catalytic activity analyses of complex **2** with DBP[A].

| Solvent | Acetone | Methanol | Ethanol | Acetonitrile | Water |
|---|---|---|---|---|---|
| Conversion of DBP (%) | 92 | 91 | 83 | 96 | 88 |
| Yield (%)[B] DPQ | 80 | 81 | 70 | 86 | 72 |
| Yield (%)[B] BQ | 8 | 6 | 10 | 7 | 11 |
| Selectivity[C] DPQ (%) | 91 | 93 | 86 | 95 | 87 |

[A]Reaction conditions: 1 mmol of DBP and $NaOCH_3$, 0.02 mmol of catalyst and 20 μL of $H_2O_2$ in 2 mL reaction medium at 45 °C; [B]Conversions and yield rates for DPQ; [C]Selectivity = ([DPQ]×100)/([DPQ] + [BQ]).

## 4 Conclusions

To sum up, two novel metal coordination complexes have been designed and synthesis through the synergetic effect of the mixed connectors. The catalytic activities of the complexes indicate that both of complexes **1** and **2** are good candidates as the catalyst for the oxidative coupling of DBP.

## Acknowledgements

We gratefully acknowledge the financial support by the key program of He'nan colleges and universities (Nos. 21B150009 and 22B530002), the He'nan Key Science and Technology Research (No. 222102320421), the He'nan Teaching Reform Program (No. 2021SJGLX881) and He'nan Educational Science Planning Program (No. 2022YB0565) and the Youth Backbone Program of Henan Vocational College of Applied Technology (No. 2022-GGJS-H005).

## References

Bai, H. Y., Ma, J. F., Yang, J., Zhang, L. P., Ma, J. C., & Liu, Y. Y. (2010). Eight two-dimensional and three-dimensional metalorganic frameworks based on a flexible tetrakis(imidazole) ligand: synthesis, topological structures, and photoluminescent properties. *Crystal Growth & Design*, 10(4), 1946-1959. http://dx.doi.org/10.1021/cg100032n.

Burrows, A. D., Fisher, L. C., Richardson, C., & Rigby, S. P. (2011). Selective incorporation of functional dicarboxylates into zinc metal–organic frameworks. *Chemical Communications (Cambridge, England)*, 47(12), 3380-3382. http://dx.doi.org/10.1039/c1cc10143a. PMid:21327218.

Chang, Z., Zhang, D. S., Hu, T. L., & Bu, X. H. (2011). Synthesis, structure and properties of microporous metal-organic frameworks constructed from Ni(II)/Cd(II), Tpt and $H_4$bpta. *Inorganic Chemistry Communications*, 14(7), 1082-1085. http://dx.doi.org/10.1016/j.inoche.2011.03.047.

Cheng, P. C., Yeh, C. W., Hsu, W., Chen, T. R., Wang, H. W., Chen, J. D., & Wang, J. C. (2012). Toward the self-assembly of metal–organic nanotubes using metal-metal and π-stacking interactions: bis(pyridylethynyl) silver(I) metallo-macrocycles and coordination polymers. *Crystal Growth & Design*, 12(2), 943-953. http://dx.doi.org/10.1021/cg201417y.

Dolomanov, O. V., Bourhis, L. J., Gildea, R. J., Howard, J., & Puschmann, H. (2010). Olex2: a complete structure solution, refinement and analysis program. *Journal of Applied Crystallography*, 42(42), 339-341.

Feng, X., Zhao, J. S., Liu, B., Wang, L. Y., Ng, S. W., Zhang, G., Wang, J., Shi, X. G., & Liu, Y. Y. (2010). A series of lanthanide-organic frameworks based on 2-Propyl-*1H*- imidazole-4,5-dicarboxylate and oxalate: syntheses, structures, luminescence, and magnetic properties. *Crystal Growth & Design*, 10(3), 1399-1408. http://dx.doi.org/10.1021/cg901391y.

Geng, J. S., Feng, W., Li, J., Tang, X. Y., Meng, L., Yu, J. P., Hu, K. Q., Yuan, L. H., Mei, L., & Shi, W. Q. (2022). Modular assembly of isostructural mixed-ligand uranyl coordination polymers based on a patterning strategy. *Inorganic Chemistry*, 61(28), 10694-10704. https://doi.org/10.1021/acs.inorgchem.2c00853.

Ghannam, J., Al Assil, T., Pankratz, T. C., Lord, R. L., Zeller, M., & Lee, W. T. (2018). A Series of 4- and 5-Coordinate Ni(II) Complexes: Synthesis, Characterization, Spectroscopic, and DFT Studies. *Inorganic Chemistry*, 57(14), 8307-8316. http://dx.doi.org/10.1021/acs.inorgchem.8b00958. PMid:29969247.

Guo, X. Z., Chen, S. S., Li, W. D., Han, S. S., Deng, F., Qiao, R., & Zhao, Y. (2019). Series of Cadmium (II) Coordination Polymers Based on a Versatile Multi-N-Donor Tecton or Mixed Carboxylate Ligands: Synthesis, Structure, and Selectively Sensing Property. *ACS Omega*, 4(7), 11540-11553. http://dx.doi.org/10.1021/acsomega.9b01108. PMid:31460260.

Hu, J. Y., Liao, C. L., & Zhao, J. A. (2012). Three Cu(II) complexes based on mixed ligands: their structures and catalytic behaviour. *Journal of Chemical Research*, 36(7), 413-417. http://dx.doi.org/10.3184/174751912X13371887324682.

Kanoo, P., Gurunatha, K. L., & Maji, T. K. (2009). Temperature-controlled synthesis of metal-organic coordination polymers: crystal structure, supramolecular isomerism, and porous property. *Crystal Growth & Design*, 9(9), 4147-4156. http://dx.doi.org/10.1021/cg900386q.

Kennemur, J. G. (2019). Poly(vinylpyridine) segments in block copolymers: synthesis, self-assembly, and versatility. *Macromolecules*, 52(4), 1354-1370. http://dx.doi.org/10.1021/acs.macromol.8b01661.

Kumar, D. K., Das, A., & Dastidar, P. (2006). One-dimensional chains, two-dimensional corrugated sheets having a cross-linked helix in metal?organic frameworks? exploring hydrogen-bond capable backbones and ligating topologies in mixed ligand systems. *Crystal Growth & Design*, 6(8), 1903-1909. http://dx.doi.org/10.1021/cg0600344.

Lan, J. W., Liu, M. S., Lu, X. Y., Zhang, X., & Sun, J. M. (2019). Novel 3D Nitrogen-Rich Metal Organic Framework for Highly Efficient $CO_2$ Adsorption and Catalytic Conversion to Cyclic Carbonates under Ambient Temperature. *ACS Sustainable Chemistry & Engineering*, 6(7), 8727-8735. http://dx.doi.org/10.1021/acssuschemeng.8b01055.

Li, M. X., Wang, H., Liang, S. W., Shao, M., He, X., Wang, Z. X., & Zhu, S. R. (2009). Solvothermal Synthesis and Diverse Coordinate Structures of a Series of Luminescent Copper(I) Thiocyanate Coordination Polymers Based on N-Heterocyclic Ligands. *Crystal Growth & Design*, 9(11), 4626-4633. http://dx.doi.org/10.1021/cg900079p.

Liu, J., Lan, Y., Yu, Z., Tan, C. S., Parker, R. M., Abell, C., & Scherman, O. A. (2017). Cucurbit[n]uril-based microcapsules self-assembled within microfluidic droplets: a versatile approach for supramolecular architectures and materials. *Accounts of Chemical Research*, 50(2), 208-217. http://dx.doi.org/10.1021/acs.accounts.6b00429. PMid:28075551.

Martins, A., Bezerra, M., Jnior, S. M., Brito, A. F., & Rangel, A. (2019). Consumer behavior of organic and functional foods in Brazil. *Food Science and Technology (Campinas)*, 40(12)

Mu, Y. J., Fu, J. H., Song, Y. J., Li, Z., Hou, H. W., & Fan, Y. T. (2011). Hydrothermal syntheses of metal–organic frameworks constructed from aromatic polycarboxylate and 4,4-Bis(1,2,4-triazol-1-ylmethyl) biphenyl. *Crystal Growth & Design*, 11(6), 2183-2193. http://dx.doi.org/10.1021/cg101494t.

Naik, A. D., Dîrtu, M. M., Léonard, A., Tinant, B., Marchand-Brynaert, J., Su, B.-L., & Garcia, Y. (2010). Engineering three-dimensional chains of porous nanoballs from a 1,2,4-triazole-carboxylate supramolecular synthon. *Crystal Growth & Design*, 10(4), 1798-1807. http://dx.doi.org/10.1021/cg901473d.

Ni, T. J., Xing, F. F., Shao, M., Zhao, Y. M., Zhu, S. R., & Li, M. X. (2011). Coordination Polymers of 1,3,5-Tris(triazol-1-ylmethyl)-2,4,6-trimethylbenzene: synthesis, structure, reversible hydration, encapsulation, and catalysis oxidation of diphenyl carbonohydrazide. *Crystal Growth & Design*, 11(7), 2999-3012. http://dx.doi.org/10.1021/cg2002749.

Pachfule, P., Das, R., Poddar, P., & Banerjee, R. (2010). Structural, Magnetic, and Gas Adsorption Study of a Two-Dimensional Tetrazole-Pyrimidine Based Metal-Organic Framework. *Crystal Growth & Design*, 10(6), 2475-2478. http://dx.doi.org/10.1021/cg1003726.

Pan, M., Lin, X. M., Li, G. B., & Su, C. Y. (2011). Progress in the study of metal–organic materials applying naphthalene diimide (ndi) ligands. *Coordination Chemistry Reviews*, 255(15-16), 1921-1936. http://dx.doi.org/10.1016/j.ccr.2011.03.013.

Qiu, Y., Li, Y., Peng, G., Cai, J., Jin, L., Ma, L., Deng, H., Zeller, M., & Batten, S. R. (2010). Cadmium metal-directed three-dimensional coordination polymers: in situ tetrazole ligand synthesis, structures, and luminescent properties. *Crystal Growth & Design*, 10(3), 1332-1340. http://dx.doi.org/10.1021/cg9013619.

Santos, I. L., Schmiele, M., Aguiar, J. P. L., Steel, C. J., Silva, E. P., & Souza, F. C. A. (2020). Evaluation of extruded corn breakfast cereal enriched with whole peach palm (bactris gasipaes, kunth) flour. *Food Science and Technology (Campinas)*, 40(2), 458-464. http://dx.doi.org/10.1590/fst.04019.

Turk, H., & Cimen, Y. (2005). Oxidation of 2,6-di-*tert*-butylphenol with *tert*- butylhydroperoxide catalyzed by cobalt(II) phthalocyanine tetrasulfonate in a methanol–water mixture and formation of an unusual product 4,4′-dihydroxy-3, 3′, 5, 5′- tetra-*tert*-butylbiphenyl. *Journal of Molecular Catalysis A Chemical*, 234(2), 19-24. http://dx.doi.org/10.1016/j.molcata.2005.02.022.

Wang, J. C., Ding, F. W., Ma, J. P., Liu, Q. K., Cheng, J. Y., & Dong, Y. B. (2015). Co(II)-MOF: a highly efficient organic oxidation catalyst with open metal sites. *Inorganic Chemistry*, 54(22), 10865-10872. http://dx.doi.org/10.1021/acs.inorgchem.5b01938. PMid:26497909.

Yang, W., Lin, X., Blake, A. J., Wilson, C., Hubberstey, P., Champness, N. R., & Schröder, M. (2009). Self-assembly of metal-organic coordination polymers constructed from a bent dicarboxylate ligand: diversity of coordination modes, structures, and gas adsorption. *Inorganic Chemistry*, 48(23), 11067-11078. http://dx.doi.org/10.1021/ic901429u. PMid:19943692.

Zhang, X., Hou, L., Liu, B., Cui, L., Wang, Y. Y., & Wu, B. (2013). Syntheses, structures, and luminescent properties of six new zinc(ii) coordination polymers constructed by flexible tetracarboxylate and various pyridine ligands. *Crystal Growth & Design*, 13(7), 3177-3187. http://dx.doi.org/10.1021/cg400579w.

Zianna, A., Psomas, G., Hatzidimitriou, A., & Lalia-Kantouri, M. (2016). Ni(II) complexes with 2,2- dipyridylamine and salicylaldehydes: synthesis, crystal structure and interaction with calf-thymus DNA and albumins. *Journal of Inorganic Biochemistry*, 163, 131-142. http://dx.doi.org/10.1016/j.jinorgbio.2016.07.003. PMid:27453533.

## Supplementary Material

Detailed structural parameters for **1** and **2** were submitted to the Cambridge Crystallographic Data Center with CCDC reference numbers 1914149 and 1914150. The crystallographic data can be acquired this free network Data Centre.

**Fig. S1.** The 1D chain of **2** (all hydrogen atoms are omitted for clarity).

**Fig. S2.** View of the 3D crystal packing of the structure of **2** (all hydrogen atoms have been omitted for clarity).

**Fig. S3.** Thermogravimetric (TG) and differential scanning calorimetric (DSC) curves for complex **1.**

**Fig. S4.** Thermogravimetric (TG) and differential scanning calorimetric (DSC) curves for complex **2.**

**Scheme S1.** Oxidation reaction of 2,6-di-tert-butylphenol.

This material is available as part of the online article from https://doi.org/10.1590/fst.88122